

ORIGINAL ARTICLE

Design and Fabrication of Natural Rubber Lightweight Spring for Motorcycle's Shock Absorber

V. Mann¹, C. Dechwayukul^{1*}, W. Thongruang¹, S. Srewaradachpisal¹, P. Kaewpradit², W. Kaew Apichai³ and H-T.Bui⁴

¹Department of Mechanical Engineering, Faculty of Engineering, Prince of Songkla University, Hat Yai, Songkhla 90112, Thailand
Phone: +6674287232; Fax: +6674558830

²Department of Chemical Engineering, Faculty of Engineering, Prince of Songkla University, Hat Yai, Songkhla 90112, Thailand

³Department of Computer Engineering, Faculty of Engineering, Prince of Songkla University, Hat Yai, Songkhla 90112, Thailand

⁴Department of Mechanical Engineering, University of Technology and Education, The University of Da Nang, Da Nang 55000, Vietnam

ABSTRACT – This research aims to design and fabricate a spring made of natural rubber for a lightweight motorcycle's shock absorber. This study is carried out in four main steps. First, a stiffness property of a steel coil spring and a damping property of a commercial shock absorber were tested using an Instron material testing machine and a test rig. Second, six different types of rubber compounds (A-1, A-2, A-3, B-1, B-2, and B-3) were formulated and the best compound was selected to use for a rubber spring. Third, the rubber spring was designed and analysed using the finite element method to investigate the best model. Finally, a prototype of the rubber spring was fabricated and tested. The steel coil spring was replaced by the rubber spring and tested for its damping property within a real shock absorber. The results of the prototype testing showed that the weight of the rubber spring was lower than the steel coil spring about 48%. The stiffness property of the rubber spring was higher than the steel coil spring around 43% and the damping property of the shock absorber using rubber spring was higher than the damping property of the shock absorber using steel coil spring about 6%. The rubber spring provided more advantages than the steel coil spring for its good corrosion resistance, lightweight, and ease of maintenance. Therefore, the implementation of the rubber spring in the real motorcycle and its fatigue life should be studied in the next future.

ARTICLE HISTORY

Revised: 27th Nov 2019

Accepted: 21st Dec 2019

KEYWORDS

Spring, Natural rubber; Steel spring; Lightweight, Shock absorber

INTRODUCTION

Using a steel coil spring could increase more weight for the vehicle. The weight of the steel coil spring was about 782 g. It was higher than the composite spring around 70% [1]. In addition, the steel coil spring was heavier than E-glass/epoxy about 26% and carbon/epoxy around 26% [2]. Another disadvantage of using the steel coil spring is the corrosion phenomenon. The corrosion led spring to be cracked or failure. The corrosion always happened at the damaged protective paint surface. This created the initial crack that would propagate to the final failure [3]. The corrosion could occur before the coating process. This corrosion broke the surface bonding between metallic and coating material, and it spread around the surface of metallic spring [4].

Many automotive industrial sectors and researchers have been interested in decreasing the weight of suspension components, especially a helical steel spring by replacing from a conventional steel spring to other alternative materials. Anil Antony Sequeira et al. [5] studied on mechanical properties of helical spring and composite spring, carbon fibre and kevlar fibre using finite element method. As a result, the helical steel spring had a higher stiffness property than carbon fibre and Kevlar fibre. However, the weight of carbon fibre and kevlar fibre was lower than helical steel spring 80% and 83% respectively. Using composite material provided benefits for saving the weight of a vehicle, but the cost of this material was very high due to its complicated manufacturing process [6].

Natural rubber is material in an elastomer group of polymers whose chemical structure contains long and regular molecule chains. Thailand has been the biggest leading in natural rubber production. In 2016, it exported natural rubber around 4.5 million tons, about 36% of world production in natural rubber [7]. Due to oversupply, the prices of Thai natural rubber have plummeted from the highest rate of around \$ 5.81 in 2011 to \$ 1.55 in 2015 [8]. As a solution, the Thai government has been offered a farmer to pay for cutting down their rubber tree and grow other crops instead [9]. Another solution, both the public and private sectors have been working together to transfer rubber raw material into finished products. Some local products were found like a rubber pillow, a protective boot, footwear, so on. This could earn three times more than selling natural rubber as the raw material [10].

A finite element method is an essential tool used to develop and design an existing and new product. It is easy to solve complex shape body, and it was capable of many analysis problems [11]. Since natural rubber has both hyperelastic and viscoelastic property, advanced material constitutive model and software tool for its non-linear characteristics need be used. Some potential tools like ABAQUS, MSC Marc/Mentat, and Ansys could be able to simulate the properties of rubber-like material. ABAQUS is a very powerful tool for finite element analysis of non-linear property of rubber-like

material with ease of use, and it is suitable for many material models. To simulate the hyperelastic property of rubber-like material, it needs to use a strain energy function. Some popular constitutive equations of hyperelasticity were the Yeoh model, the Ogden model, the Neo-Hooke model, the Mooney-Rivlin model, etc. [12]. To calibrate the material parameters of the models, the uniaxial, biaxial and planar test was used [13, 14]. Marvalova [15] has used the Bergstrom Boyce model (BB model) to study the viscoelastic property of filled rubber. The model was fitted well between simulation and experiment. Hamid et al. [16] have compared the Bergstrom Boyce model with the Prony series for Yeoh viscoelasticity. As a result, the BB model showed a good agreement than the Prony series in medium strain. Bergstrom Boyce model consisted of two networks (figure 1). Network A represented the equilibrium state response of the material (hyperelasticity) and network B represented the time-dependent deviation from the equilibrium state (non-linear viscoelasticity) [17, 18, 19]. To calibrate the material parameters of BB model, Mcalibration® software was used. This software could calibrate parameters of many material constitutive models such as a hyperelastic and viscoelastic material, etc. The software was easy to use. The parameters of the material model have generated automatically from the software. A user could save the result from the calibration in different formats to use in various finite element analysis software [20].

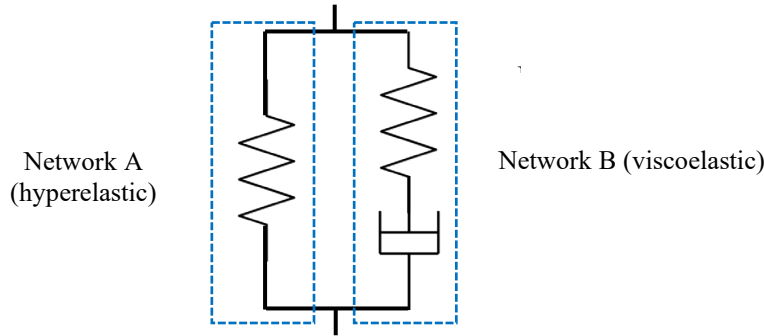


Figure 1. Symbolic representation of the BB model.

Network (A), the model is expressed in a hyperelastic property. Some hyperelastic constitutive models are Yeoh model, Ogden model and Neo-Hookean model. The Yeoh model is in Eq. (1).

$$U = \sum_{i=1}^3 C_{i0}(I_1 - 3)^i \tag{1}$$

Where, U is a strain energy function, C_{i0} is material constant, and I_1 is a first deviatoric strain invariant. The Ogden model is:

$$U = \sum_{i=1}^N \frac{2\mu_i}{\alpha_i^2} (\bar{\lambda}_1^{\alpha_i} + \bar{\lambda}_2^{\alpha_i} + \bar{\lambda}_3^{\alpha_i} - 3) \tag{2}$$

Where, U is a strain energy function, N is a material parameter, μ_i, α_i^2 is material parameters in temperature-dependence and $\bar{\lambda}_i^{\alpha_i}$ is deviatoric principal stretches. The Neo-Hookean model is:

$$U = C_{10}(I_1 - 3) \tag{3}$$

Where is U is a strain energy function, C_{10} is a material constant and I_1 is a first deviatoric strain invariant. Network (B), the model is represented in a power creep law.

$$\dot{\epsilon}_B = A[\lambda_B - 1]^C (\sigma_B)^m \tag{4}$$

Where, $\dot{\epsilon}_B$ is effective creep strain rate, A is dimensional consistency, $\lambda_B - 1$ is normal creep stain, C is creep strain dependence ($C = [-1,0]$), σ_B is effective stress and m is effective stress dependence ($m > 1$).

Besides the functions raised above, the stress ratio performed by the network (B) to the stress performed by the network (A) under instantaneous loading, S is also defined. Sagar et al. [21] have developed a test rig to study a damping property of shock absorber. The test rig consisted of load cell at the top side, displacement transducer at the bottom side of the shock absorber and D.C motor was connected to a control unit. A lot of researchers have been invented many lightweight springs from different kinds of material, but those components were not made of natural rubber. Furthermore, natural rubber was used in many applications; however, it was not yet used in automotive shock absorber, especially a coil spring.

The purpose of this research is to design and fabricate a lightweight spring for motorcycle's shock absorber from natural rubber. This study is motivated by the need for a lightweight spring for a vehicle's shock absorber and a value-add of natural rubber for farmers who have been hurt by a drop in global price. There are four main targets in this work. First, the stiffness of the steel coil spring and the damping property of shock absorber are tested using an Instron material testing machine model 8872 and a test rig. Second, the natural rubber compound is formulated to obtain the best properties. Third, the rubber spring was designed and analysed using the finite element method to investigate the best model. Finally, the prototype is fabricated and tested. The mechanical properties of the spring made of natural rubber are compared with the steel coil spring.

METHODS

The procedure of the research is divided into four steps. First, testing stiffness of steel coil spring and damping property of the shock absorber is carried out. Second, a rubber material is formulated to get the best compound. Third, the spring made of natural rubber is designed and analysed using the finite element method to obtain the best model. Finally, the prototype of natural rubber spring is fabricated and tested.

Testing Stiffness of Steel Coil Spring and Damping Property of Shock Absorber

A commercial steel coil spring has 145 mm in height, 52 mm in outside diameter and 32 mm in inside diameter. A steel coil spring (figure 2) is compressed 20mm using an INSTRON® material testing machine model 8872(25KN). Its stiffness property K is defined from a force and displacement relationship (figure 3) using Hooke's Law. A force and displacement curve of the steel coil spring from the compression test using INSTRON model 8872(25KN) is illustrated in Figure 3. Based on a force and displacement relationship, the stiffness constant of the steel coil spring is 42,596 N/m. Damping property of the shock absorber using steel coil spring is tested using the test rig (Figure 4). A test rig consists of a 3hp electric motor single phase and it is linked to a cam through its shaft. The cam is indirectly connected to a shock absorber by a follower. The shock absorber was compressed under a harmonic force with 60 rpm of motor speed for 60 seconds. The force and time were recorded by a force sensor which was attached at the top side of the shock absorber.

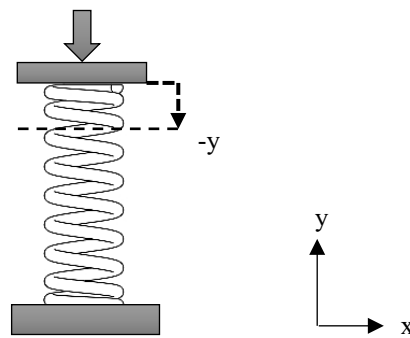


Figure 2. Free body diagram of the steel coil spring under compression.

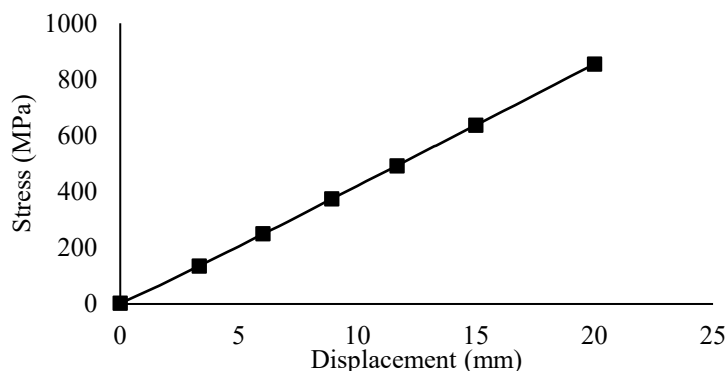


Figure 3. Force and displacement curve of the steel coil spring under compression.

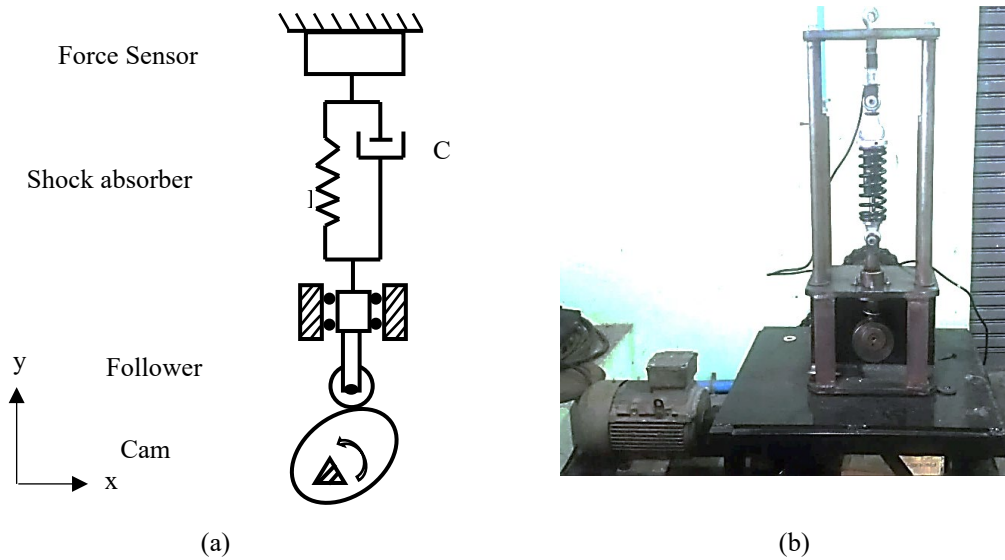


Figure 4. Free body diagram of shock absorber test rig(a) and test rig machine (b).

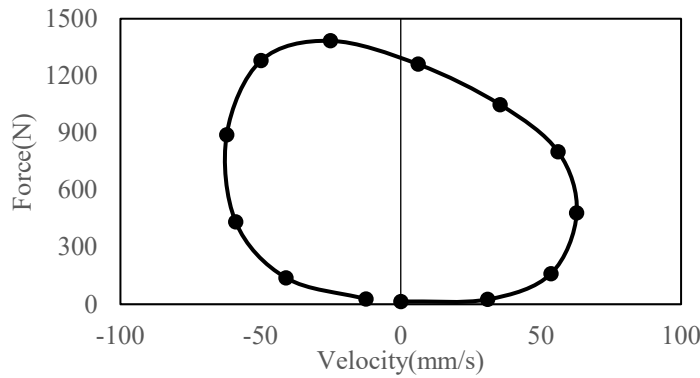


Figure 5. Force and velocity curve of the shock absorber with steel coil spring from test rig.

Figure 5 shows a curve profile of the force and displacement relationship of the shock absorber using steel coil spring from the test rig. The damping property of the shock absorber using the steel coil spring is defined by Eq. (5).

$$\text{Damping coefficient, } D(t) = \frac{F(t)}{v(t)} \tag{5}$$

Where D(t) refers to the damping coefficient (Ns/m), F(t) refers to the force (N) recorded from the load cell, and v(t) refers to the velocity (m/s) calculated from the cam-follower Eq. (6).

$$x'(t) = v(t) = \frac{20\pi \cos\left(2\pi t - \frac{\pi}{2}\right) + \frac{1}{2}(400\pi \cos\left(2\pi t - \frac{\pi}{2}\right) \sin\left(2\pi t - \frac{\pi}{2}\right)}{\sqrt{42.5^2 - 10^2(1 - \sin^2\left(2\pi t - \frac{\pi}{2}\right))}} \tag{6}$$

Rubber Formulation

There are six different rubber compounds formulated, as shown in Table 1. Natural rubber (STR 5L) and other chemical compositions are used in the compounds including steric acid, zinc oxides, wing stay L, paraffin oil, MTB (2-Mercaptobenzothiazole), sulfur, carbon black N330, Silica, and CaCO₃. Natural rubber and other additive substances are mixed using a two-roll mill machine about 30 minutes and cured with a hydraulic hot press machine under the temperature of 150°C for 20 minutes.

Two mechanical material testing like uniaxial compression and cyclic loading were carried out. The uniaxial compression test has followed the standard of ASTM D575 method A [22]. For the cyclic loading test, filled vulcanized natural rubber specimens are performed the loaded and unloaded testing for five times under a load cell of 2.5KN using a material testing machine Zwick Roell, Germany (Z010).

Table 1. Rubber compounding for natural rubber spring.

| No. | Chemical compositions (Phr.) | A-1 | A-2 | A-3 | B-1 | B-2 | B-3 |
|-----|------------------------------|-----|-----|-----|-----|-----|-----|
| 1 | NR | 100 | 100 | 100 | 100 | 100 | 100 |
| 2 | ZnO | 5 | 5 | 5 | 5 | 5 | 5 |
| 3 | Wingstay L | 1 | 1 | 1 | 1 | 1 | 1 |
| 4 | Steric acid | 1.5 | 1.5 | 1.5 | 1.5 | 1.5 | 1.5 |
| 5 | Carbon black (CB-N330) | 60 | - | - | 30 | 30 | - |
| 6 | Silica | - | 60 | - | 30 | - | 30 |
| 7 | CaCO ₃ | - | - | 60 | - | 30 | 30 |
| 8 | Paraffin oil | 2 | 2 | 2 | 2 | 2 | 2 |
| 9 | MBT | 1 | 1 | 1 | 1 | 1 | 1 |
| 10 | Wing Stay L | 1.5 | 1.5 | 1.5 | 1.5 | 1.5 | 1.5 |
| 11 | Sulfur | 2 | 2 | 2 | 2 | 2 | 2 |

Design and Simulation

Structure design for natural rubber spring

The rubber spring is designed to be fabricable by rubber moulding and machining. It should also be easy to install in different kinds of motorcycles. The rubber spring consists of six aluminium plates and five rubber pads. The aluminium is used in this design because of its advantage in a lightweight, good in thermal conductivity, low cost, and ease of machining. Using aluminium material with rubber pad could also improve the stiffness of the rubber spring. Figure 6 illustrates three models of rubber spring. Different models of rubber spring have the different shapes. The rubber spring model-1 has a cylindrical shape (as in Figure 6(a)), model-2 has a biconcave shape (as in Figure 6(b)), and model-3 has a biconvex shape (as in Figure 6(c)). Each type of rubber cell has the same thickness of 24 mm, an inner diameter of 40mm, and a maximum outer diameter of 60 mm. The aluminium plate has a thickness of 3 mm, an outer diameter of 64mm, and an inner diameter of 40 mm for all models.

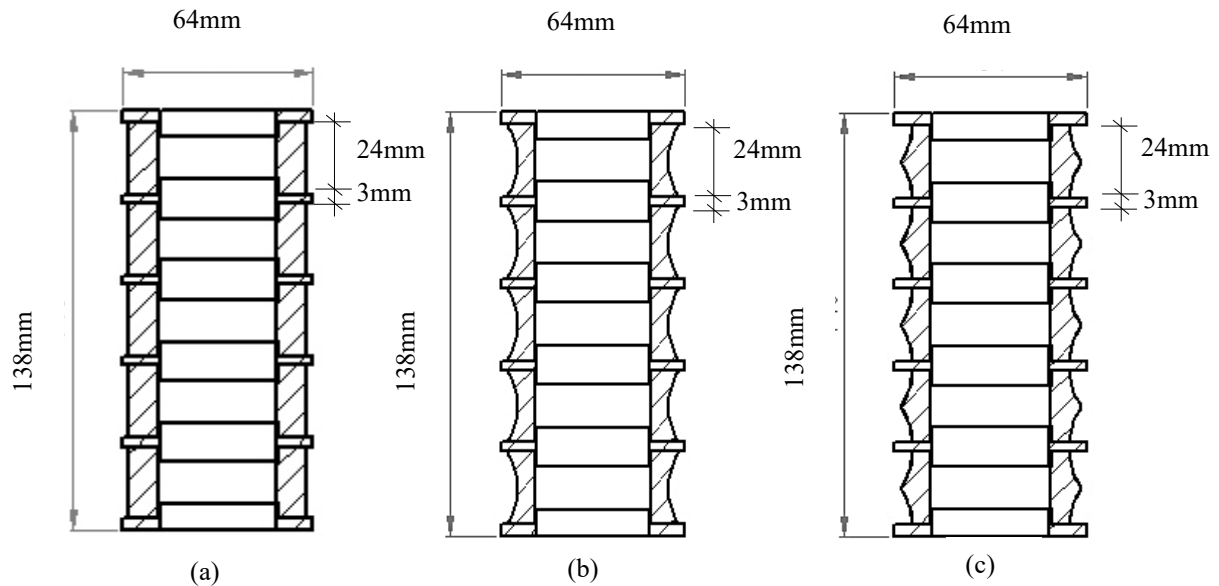


Figure 6. Rubber spring (a) model-1, (b) model-2 and (c) model-3.

Hyperelastic simulation for natural rubber spring

The mechanical property including stiffness and damping property of rubber spring is analysed by the finite element method (FEM) using Abaqus® CAE 6.13 because it is able to simulate the non-linear viscoelasticity model, Bergstrom Boyce model, with ease of use. The natural rubber used in this study is assumed to be isotropic and incompressible material. Hyperelastic constitutive model Yeoh is chosen to be used because of its good fit for a large strain with the limited experimental data [23]. The material parameters of hyperelastic Yeoh are obtained from Mcalibration® software version 4.2.0 developed by Veryst Engineering, LLC. This software is very potential to calibrate different kinds of the material constitutive model with the less requirement of the experimental test. Due to the limitation of the testing equipment, only the uniaxial compression test is used in this study. Figure 7 shows material parameter calibration of the Yeoh model using Mcalibration® software version 4.2.0 with the coefficient of determination $R^2 = 0.994$. The material parameters of the Yeoh model are listed in table 2.

Aluminium 7075-T651 has the mass density (ρ) of $2.81 \times 10^3 \text{ Kg/m}^3$, elastic modulus (E) of $70 \times 10^3 \text{ MPa}$ and Poisson’s ratio (ν) of 0.32 [24]. Rubber pads of each model are interacted with aluminium plates by surface-to-surface contact (standard) with a friction coefficient (μ) of 0.8 [25]. The constraint method XSYMM ($U1 = UR2 = UR3 = 0$) is

used for the axisymmetric model of rubber spring (figure 8). The bottom side of the rubber spring structure is constrained by ENCASTRE ($U_1 = U_2 = U_3 = UR_1 = UR_2 = UR_3 = 0$). The displacement control method is used in the analysis. The top side of the rubber spring is compressed 20mm, and the force is recorded. The geometry of rubber pads and aluminium plates are discretized into a 4-node bilinear axisymmetric quadrilateral, hybrid, constant pressure (CAX4H). Model-1 contains 532 elements and 1159 nodes. Model-2 has 419 elements and 923 nodes. Model-3 comprises 388 elements and 846 nodes. The simulation is used as a geometric nonlinearity approximation to the total stiffness matrix.

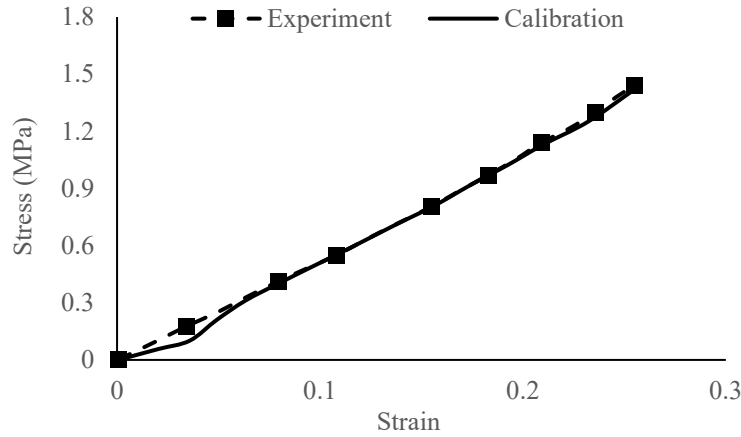


Figure 7. Material parameters calibration for Hyperelastic constitutive model (Yeoh model) using Mcalibraton® software version 4.2.0.

Table 2. Material parameters of Yeoh model.

| Material model | Material Parameter | | |
|----------------------|--------------------|-------------|-------------|
| Yeoh hyperelasticity | C10 = 0.574 | C20 = 0.122 | C30 = 0.023 |
| | D1 = 0 | D2 = 0 | D3 = 0 |

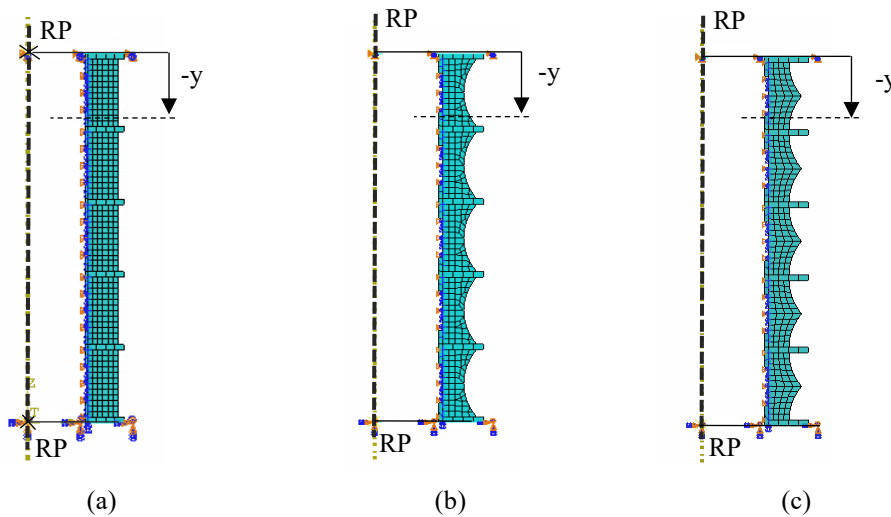


Figure 8. The boundary condition of rubber spring model-1 (a), rubber spring model-2 (b), and rubber spring model-3 (c) for hyperelastic simulation.

Non-Linear viscoelastic simulation for spring made of natural rubber

Since the property of natural rubber is non-linear viscoelastic, Bergstrom Boyce model (BB model) is used in this simulation. The material parameters of the BB model are calibrated by Mcalibraton® software version 4.2.0. The load-unloading compression test of the specimen with 28 mm in diameter and 12 mm in height at two different strain rates (-0.1/s and -1.0/s) under 25% strain is carried out for material calibration[26]. Figure 9 represents the material parameters of the non-linear viscoelastic material model (Bergstrom Boyce) calibrated by Mcalibraton software version 4.2.0 with the coefficient of determination $R^2 = 0.964$. The material parameters from the calibration are listed in Table 3.

Table 3. Material parameters of Bergstrom Boyce model calibrated from Mcalibration® software.

| Bergstrom Boyce material parameters | | | | |
|-------------------------------------|------------|------------|-------------|----------|
| Yeoh model | C10 = 0.25 | C20 = 1.43 | C30 = -1.15 | |
| | D1 = 0.0 | D2 = 0.0 | D3 = 0.0 | |
| Power creep law | S = 1.65 | A = 1.30 | m = 2.50 | C = -1.0 |

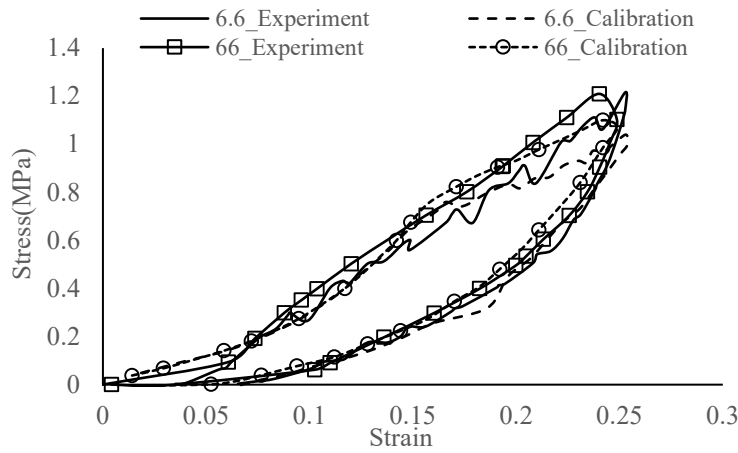


Figure 9. Material parameters calibration for non-linear viscoelastic constitutive model (BB model) using Mcalibration software version 4.2.0.

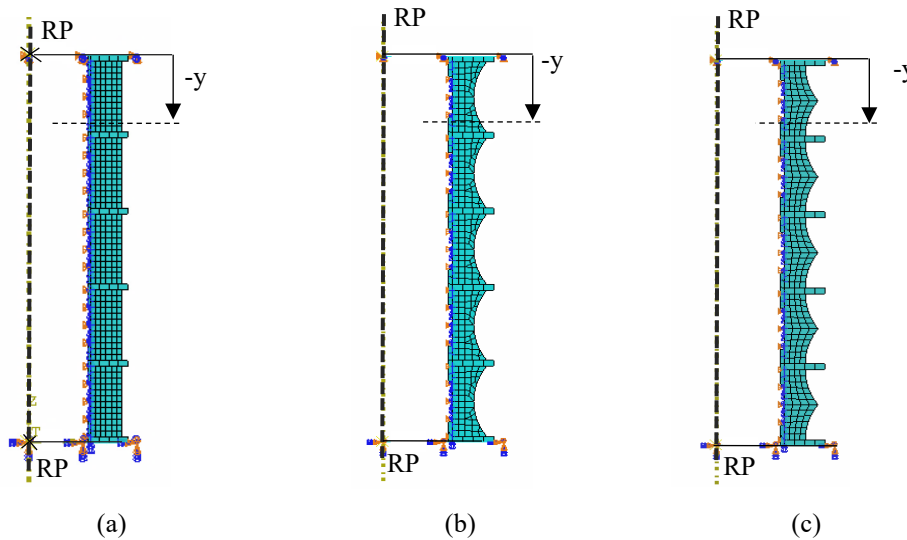


Figure 10. Boundary condition of rubber spring model-1(a), rubber spring model-2(b), and rubber spring model-3 (c) for non-linear viscoelastic simulation.

The constraint XSYMM ($U1 = UR2 = UR3 = 0$) is used for the 2D axisymmetric rubber spring. The bottom side of the rubber springs are constrained by ENCASTRE ($U1 = U2 = U3 = UR1 = UR2 = UR3 = 0$). The displacement control method is used in the simulation. The top side of the rubber spring is compressed 20 mm, and the force was recorded. The rubber pads are connected to the aluminium plates by surface-to-surface contact (standard) with a friction coefficient (μ) of 0.8. The dashpot element is connected between the top and bottom reference points of the rubber spring. The simulation is used as a non-linear geometry approximation to the total stiffness matrix. The rubber pads and aluminium plates (figure 10) are discretized into a 4-node bilinear axisymmetric quadrilateral, hybrid, constant pressure (CAX4H). There are 532 elements and 1159 nodes for model-1, 419 elements and 923 nodes for model-2 and 388 elements and 846 nodes for model-3. The simulation is used as a geometric nonlinearity approximation to the total stiffness matrix.

Prototype Making and Testing

The rubber pads were fabricated using a compression moulding by the hydraulic hot press machine. The rubber compound was vulcanised for 20 minutes under a temperature of 150 °C in the prepared mould. The spring made of natural rubber was tested for its stiffness property using Instron material testing machine model 8872 (figure 11a). The steel coil spring is replaced by the spring made of natural rubber and tested to find the damping characteristic using the shock absorber test rig as shown in Figure 11(b). A commercial shock absorber used in the test is model YSS G-series for Honda MSX (MC302-250TL-19-5). It is a single tube filled hydraulic shock absorber with a total length of 250 mm.

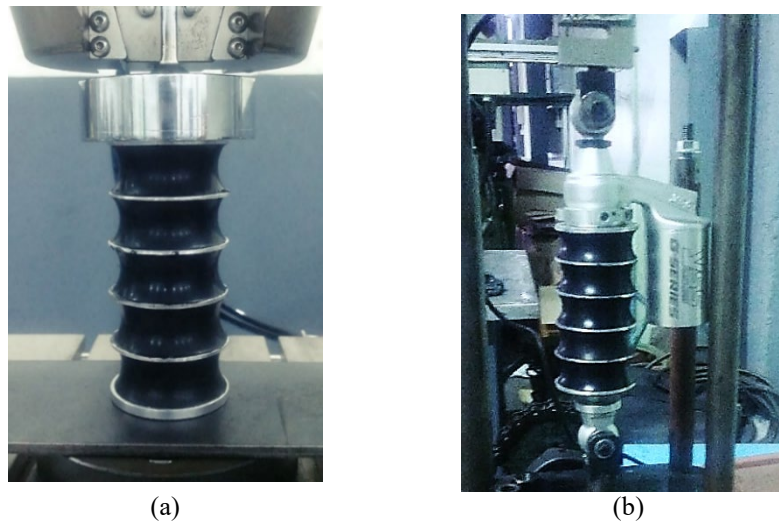


Figure 11. (a) Rubber spring under compression using Instron machine and (b) testing of shock absorber with rubber spring using test rig.

RESULTS & DISCUSSION

Result of Rubber Formulation

Figure 12 illustrates the stress and strain relationship of elastic modulus and hysteresis loop for six different rubber compounds. Figure 12(a) represents a modulus of elasticity of six rubber compounds. Based on the result, compound A-1 shows a higher elastic modulus while the other compound shows a similar property. Figure 12(b) describes the hysteresis loop of six rubber compounds. Compound A-1 provides the biggest hysteresis loop than the other five compounds.

The mechanical property like modulus of elasticity and hysteresis loss ratio are listed in Table 4. The elastic modulus of compound A-1 is 6.81 MPa; compound A-2 is 2.21 MPa, compound A-3 is 3.05 MPa, compound B-1 is 3.90 MPa, compound B-2 is 3.01 and compound B-3 is 3.05. Furthermore, the hysteresis loss ratio of compound A-1, A-2, A-3, B-1, B-2 and B-3 are 0.43, 0.32, 0.37, 0.42, 0.40 and 0.36 respectively.

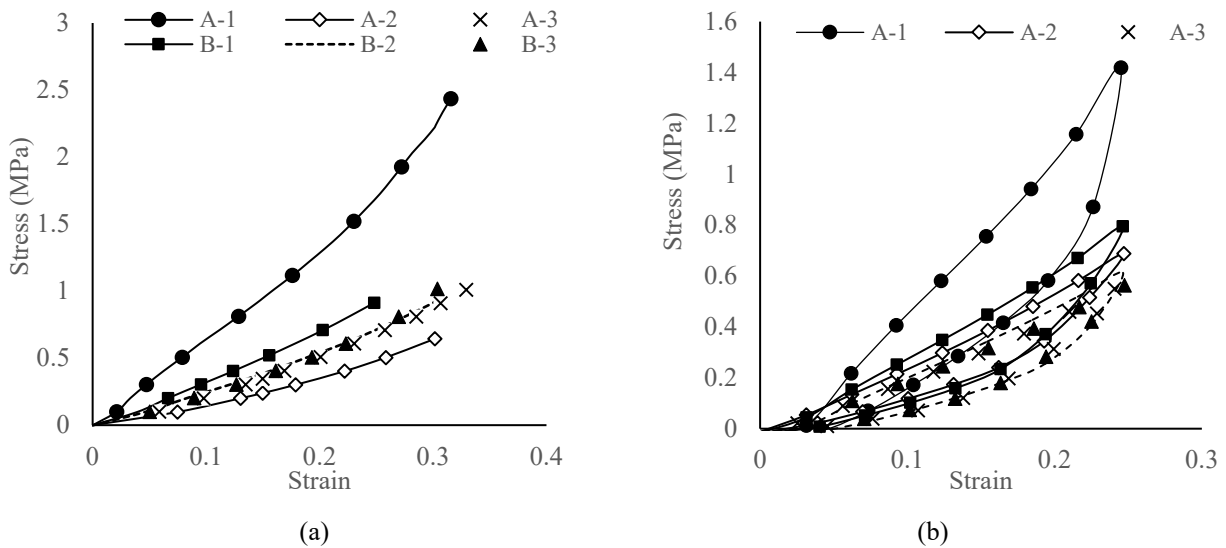


Figure 12. (a) Stress-strain relationship of different rubber compounds and (b) hysteresis loop of different rubber compounds.

Table 4. Modulus of elasticity and hysteresis loss ratio for different rubber compounds.

| Compound | Modulus of elasticity (MPa) | Hysteresis loss ratio |
|----------|-----------------------------|-----------------------|
| A-1 | 6.81 | 0.43 |
| A-2 | 2.21 | 0.32 |
| A-3 | 3.05 | 0.37 |
| B-1 | 3.90 | 0.42 |
| B-2 | 3.01 | 0.40 |
| B-3 | 3.05 | 0.36 |

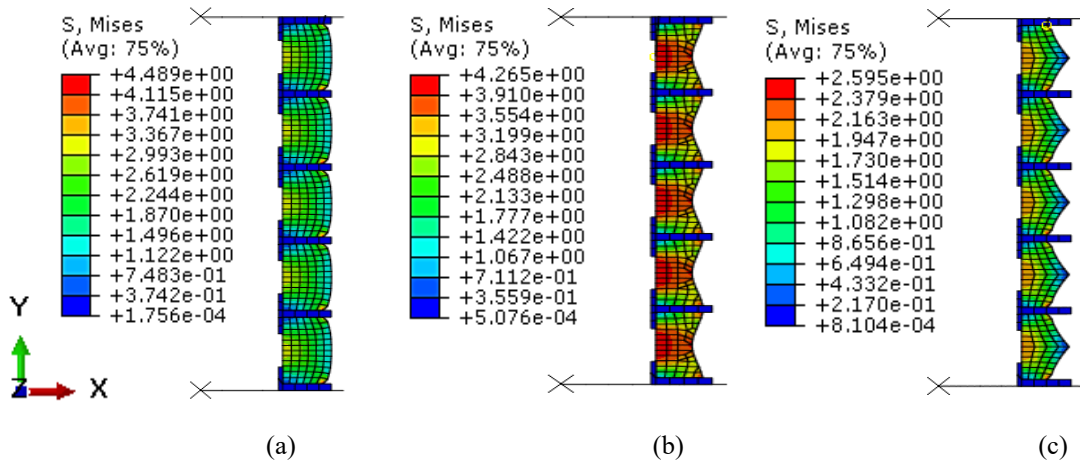


Figure 13. Mises stress distribution in the hyperelastic simulation of (a) rubber spring model-1, (b) rubber spring model-2, and (c) rubber spring model-3.

Table 7. Maximum stress value of rubber spring from hyperelastic simulation.

| Model No. | Mises(MPa) | S11(MPa) | S22(MPa) | S33(MPa) |
|-----------|------------|----------|----------|----------|
| Model-1 | 4.49 | 3.36 | 1.37 | 1.56 |
| Model-2 | 4.26 | 3.57 | 0.64 | 1.32 |
| Model-3 | 2.59 | 1.63 | 0.19 | 0.74 |

Figure 13 shows the result of hyperelastic simulation for three different types of rubber springs such as model-1 in 13(a), model-2 in 13(b), and model-3 in 13(c). Table 7 represents the maximum stress for each model of rubber spring. The mises stress, S11 stress (principle stress in the x-direction), S22 (principle stress in the y-direction), and S33 stress (principle stress in the z-direction) are shown in the unit of MPa. The rubber spring model-1 has the highest stresses, and this followed by model-2 and model-3.

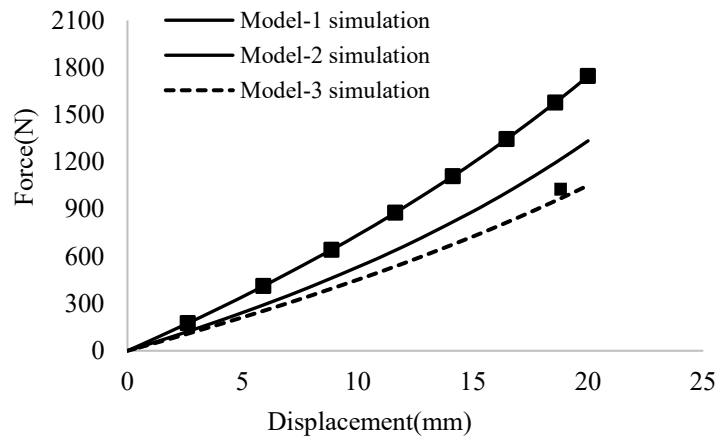


Figure 14. Force and displacement relationship for rubber spring with different model from hyperplastic simulation and steel coil spring from testing.

Figure 14 illustrates a force and displacement relationship of three different rubber spring from the simulation. Rubber spring model-1 shows the highest stiffness modulus, and it is followed by model-2 and model-3. Table 5 lists a stiffness property of rubber spring. The stiffness constant of rubber spring model-1 is 81,711 N/m, model-2 is 61,663 N/m and model-3 is 49,845 N/m.

Table 5. Stiffness coefficient of natural rubber spring for three models and steel spring.

| Rubber spring | Stiffness (N/m) |
|-----------------------|-----------------|
| Rubber spring model-1 | 81,711 |
| Rubber spring model-2 | 61,663 |
| Rubber spring model-3 | 49,845 |

Result of Non-Linear Viscoelastic Simulation

Figure 15 shows the result of non-linear viscoelastic simulation for three different types of rubber springs such as model-1 (13a), model-2(13b), and model-3(13c). Table 6 represents the maximum stress for each model of rubber spring. The mises stress, S11 stress (principle stress in the x-direction), S22 (principle stress in the y-direction), and S33 stress (principle stress in the z-direction) are shown in the unit of MPa. The rubber spring model-1 has the highest stresses than model-2 and model-3 for mise stress, S22 stress, and S33 stress. However, model-3 has higher S11 stress than the other model.

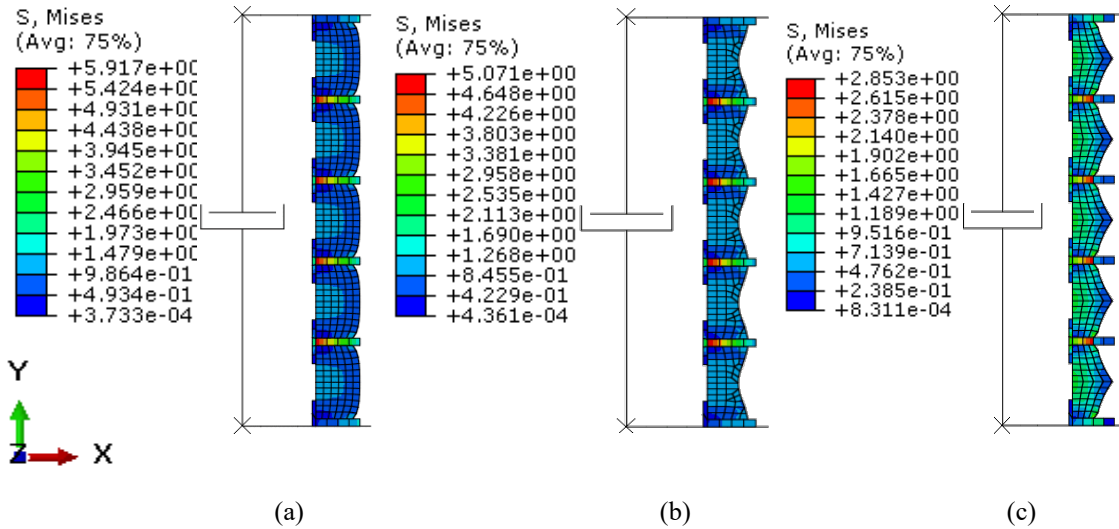


Figure 15. Stress distribution in (a) rubber spring model-1, (b) rubber spring model-2 and (c) rubber spring model-3 from a non-linear viscoelastic simulation.

Table 6. Maximum stress value of rubber spring from non-linear viscoelastic simulation.

| | Mises (MPa) | S11 (MPa) | S22 (MPa) | S33 (MPa) |
|---------|-------------|-----------|-----------|-----------|
| Model-1 | 5.91 | 4.63 | 1.58 | 2.03 |
| Model-2 | 5.10 | 4.24 | 1.00 | 1.57 |
| Model-3 | 2.85 | 13.23 | 1.00 | 0.87 |

Figure 16 explains the damping property of three rubber spring. From the force and velocity relationship curve, rubber spring model-1 has the biggest damping loop. This is followed by rubber spring model-2 and model-3. Table 7 represents the damping, stiffness to weight ratio and damping to weight ratio of rubber spring of each rubber spring from the simulation. The damping coefficient for rubber spring model-1 is 165,640Ns/m, model-2 is 128,032 Ns/m, and model-3 is 46,140 Ns/m. The rubber spring model-1 has a damping coefficient more than rubber spring model-2 and model-3. The rubber spring model-2 has higher stiffness to the weight ratio and damping to weight ratio than rubber spring model-1 and rubber spring model-3. For this reason, the rubber spring model-2 is selected as a prototype to be fabricated and tested.

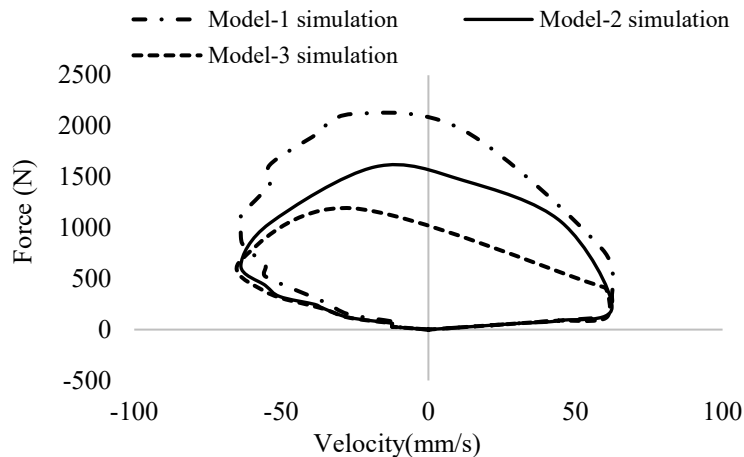


Figure 16. Force and velocity relationship for rubber spring with different model from non-linear viscoelastic simulation.

Table 7. Damping coefficient, stiffness to weight ratio and damping to weight ratio of three rubber spring models.

| Rubber spring | Damping property (Ns/m) | Stiffness to weight ratio | Damping to weight ratio |
|-----------------------|-------------------------|---------------------------|-------------------------|
| Rubber spring model-1 | 165,640 | 194 | 392 |
| Rubber spring model-2 | 128,032 | 196 | 410 |
| Rubber spring model-3 | 46,140 | 160 | 148 |

Result of Rubber Spring Model-2 from Simulation and Experiment

Figure. 17(a) and 17(b) represents the stiffness property and damping property of the rubber spring model-2 from the testing and simulation. The result shows in good agreement between the experiment and simulation. The percentage of error between simulation and experiment for stiffness property is around 13.64%, and for damping property, the difference is about 9.81 %.

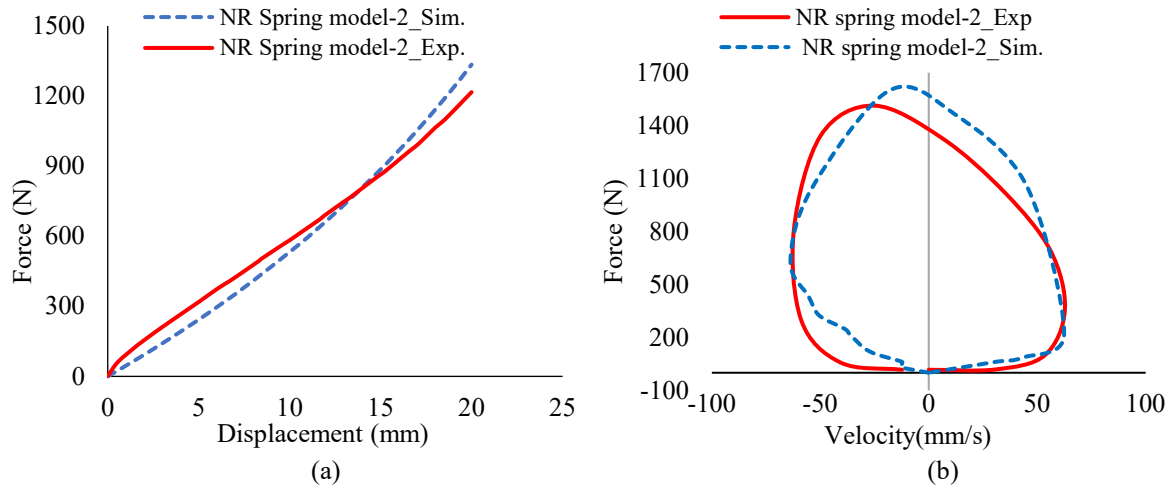


Figure 17. (a). Stiffness property of natural rubber spring model-2 from simulation and experiment and (b) damping property of rubber spring model-2 with dashpot of shock absorber from simulation and experiment.

Comparison of Rubber Spring Model-2 And Steel Coil Spring from Experiment

Figure. 18 shows the stiffness property of the rubber spring and steel coil spring and damping property of the shock absorber using rubber spring and steel coil spring from the experiment. The damping and stiffness property of rubber spring model-2 is higher than the steel coil spring. Table 8 shows the comparison of stiffness and damping coefficient of the rubber spring model-2 and steel coil spring. The stiffness constant of the rubber spring model-2 is 60,759 N/m while the stiffness constant of the steel coil spring is 42,597 N/m. The damping coefficient of shock absorber using rubber spring model-2 is 216,457Ns/m and the damping coefficient of shock absorber using steel coil spring is 203,532 Ns/m. The percentage of difference between rubber spring model-2 and steel coil spring for stiffness property is about 42.63% and for damping property, the difference is about 6.35%.

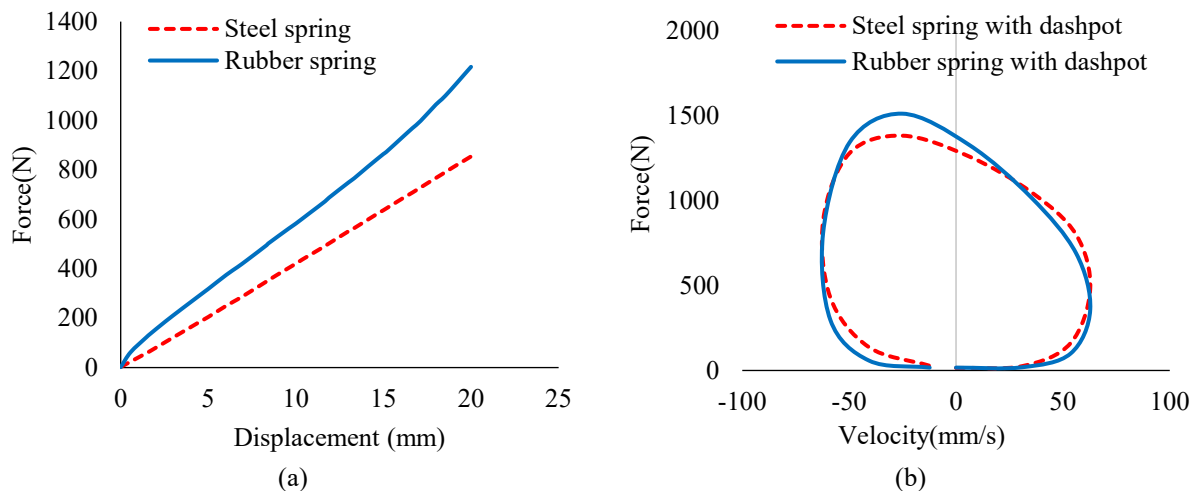


Figure 18. (a) Stiffness property of rubber spring and steel coil spring and (b) damping property of shock absorber using rubber spring and steel coil from experimental testing using the test rig.

Figure. 19 illustrates the weight of the natural rubber spring and the steel coil spring. The spring made of natural rubber weights 239 g and the steel coil spring weights 458 g. Table 9 represents the comparison of stiffness to weight ratio and damping to weight ratio between rubber spring model-2 and steel coil spring. The stiffness to weight ratio for rubber spring model-2 is about 259 and for steel coil spring is about 93. Also, the damping to weight ratio for rubber spring model-2 is around 906 and for steel coil spring, the ratio is around 444. In conclusion, the rubber spring model-2 has higher stiffness and damping to weight ratio than the steel coil spring.

Table 8. Stiffness property of rubber spring and steel coil spring and damping property of shock absorber using rubber spring and steel coil spring.

| Property | Rubber spring model-2 | Steel coil spring | Difference (%) |
|-----------------|-----------------------|-------------------|----------------|
| Stiffness (N/m) | 60,759 | 42,597 | 42.63 |
| Damping (Ns/m) | 216,457 | 203,532 | 6.35 |

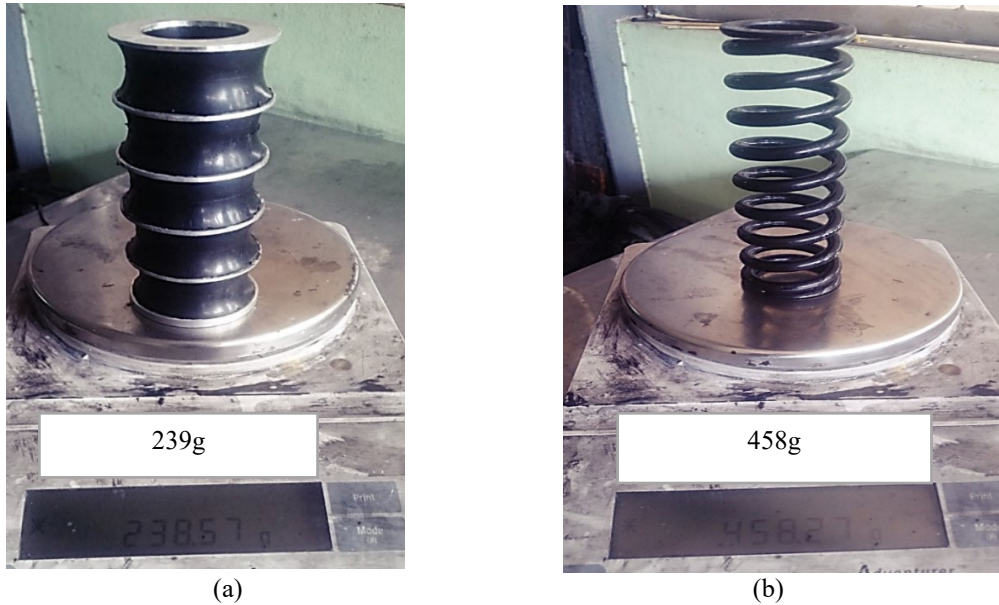


Figure 19. (a) Weight of spring made of natural rubber and (b) weight of steel coil spring.

Table 9. Stiffness to weight ratio and damping to weight ratio of rubber spring model-2 and steel coil spring from experiment.

| | Rubber spring model-2 | Steel coil spring |
|---------------------------|-----------------------|-------------------|
| Stiffness to weight ratio | 259 | 93 |
| Damping to weight ratio | 906 | 444 |

CONCLUSION

The purpose of this research is to design and fabricate a lightweight rubber spring for the motorcycle. Based on the result of the experiment, the weight of the rubber spring is lower than the steel coil spring about 48%. The stiffness property of the rubber spring and steel coil spring is different around 43% and the damping of shock absorber using rubber spring and steel coil spring is different about 6%.

The rubber material is formulated to get the desired mechanical properties. According to the experimental result, the compound A-1 provides the best mechanical properties compared to compound A-2 and A-3. Therefore, the rubber compound A-1 is selected to be used in the design of the rubber spring. Three models of rubber spring are designed and simulated using finite element analysis. Based on the comparison of stiffness to weight ratio and the damping to weight ratio of each model of rubber spring, the rubber spring model-2 provides more advantage than the rubber spring model-1 and model-2. For this reason, the rubber spring model-2 is selected as a prototype to be fabricated and tested. The results show a good agreement between experiment and simulation.

The shock absorber using rubber spring should be applied in the real motorcycle, and the fatigue test for rubber spring should also be studied in the next future. The rubber spring provides some advantages over steel coil spring such as:

- i. It has a lower weight than the steel coil spring about 48%.
- ii. It has a high corrosion resistance because it is made of rubber and aluminium.
- iii. It is easy to install and maintain. When any rubber pad is cracked or broken, it can be replaced by just a single piece of a rubber pad or aluminium plate.

In conclusion, the rubber spring has many benefits compared to the steel coil spring. It is practical and can be used as an alternative spring for shock absorber.

ACKNOWLEDGEMENT

Authors would like to express their gratitude for the Department of Mechanical Engineering, Faculty of Engineering, Prince of Songkhla University for its laboratory facilitation. The research has been funded by the Faculty of Engineering, Prince of Songkhla University, under grant number ENG-61-2-7-16-02395.

REFERENCES

- [1] Rajaram MS, Soham PG, Suresh MS. Comparison of weights of steel and composite coil spring for two wheeler suspension systems. In: 4th RIT Post Graduates Conference, Maharashtra, India, pp. 13-16; April, 2018.
- [2] Sujit SP, Subodh K, Shubham S. Comparative study of helical compression suspension spring for different materials. *Asian Journal of Engineering and Applied Technology*, 2016; 5(2): 22-28.
- [3] Goran V, Marino B. Failure analysis of a motor vehicle coil spring. In: 21st European Conference on Fracture, Catania, Italy, pp. 2944–2950; June, 2016, doi: 10.1016/j.prostr.2016.06.368.
- [4] Alejandro PH. An investigation of automotive springs: ageing effects. A thesis submitted to The University of Manchester for the degree of Master of Philosophy in the Faculty of Sciences & Engineering; 2016: 86-88.
- [5] Anil AS, Ram KS, Ganesh KS. Comparative analysis of helical steel springs with composite springs using finite element method. *Journal of Mechanical Engineering and Automation*, 2016; 6(5): 63-70.
- [6] Yahya K. A review: Fibre reinforced polymer composite helical springs. *Journal of Materials Science & Nanotechnology* 2017; 5(1): 1-6.
- [7] Business Wire. Rubber manufacturers in Thailand-BizVibe announces a new B2B networking platform for the rubber industry in Thailand. Retrieved from <https://bwnews.pr/37yXs3R>; 25 August, 2019.
- [8] Suphanida Th. Thai rubber farmers plan protest over low prices, seek aid. Retrieved from <https://reut.rs/2sdgTz6>; 24 November, 2019.
- [9] Thakral S. Thai rubber farmers plan protest over low prices, seek aid. Retrieved from <https://reut.rs/34KPvq7>; 24 November, 2019.
- [10] Theparat C. Rubber farm cut aimed to buoy price. Retrieved from <https://bit.ly/2KRfAMF>; 24 November, 2019.
- [11] Daryl LL. A First course in the finite element method. 6th ed. Ohio: Cengage Learning, Inc; 2018.
- [12] Piotr S, Łukasz J. Selection of a hyper-elastic material model – a case study for a polyurethane component. *Latin American Journal of Solids and Structures*, 2019; 16(5): 1-16.
- [13] Smith M. ABAQUS/Standard User's Manual, Version 6.13: Hyperelastic behavior of rubber. Retrieved from <https://bit.ly/2rib0jD>; 25 November, 2019.
- [14] Marckmann G, Verron E. Comparison of hyperelastic models for rubber-like materials. *Rubber Chemistry and Technology*, 2006; 79(5): 835-858.
- [15] Marvalova B. Viscoelastic properties of filled rubber. *Experimental Observations and Material Modelling*, 2007; 14 (1-2): 81-89.
- [16] Mir HRG, Mohammad A, et al. Modeling the hyperviscoelastic behavior of a tire tread compound reinforced by silica and carbon black. *Journal of Applied Polymer Science*, Wiley Periodicals, Inc, 2013; 128: 1725–1731.
- [17] Bergström JS, Boyce MC. Constitutive modeling of the time-dependent and cyclic loading of elastomers and application to soft biological tissues. *Journal of Mechanics and Materials*, 2001; 33: 523-530.
- [18] Bergström JS, Boyce MC. Large strain time-dependent behavior of filled elastomers. *Journal of Mechanics and Material*, 2000; 32: 627-644.
- [19] Smith M. ABAQUS/Standard User's Manual, Version 6.13: Hysteresis in elastomers. Retrieved from <https://bit.ly/2OEZiHL> ; 25 November, 2019
- [20] Veryst Engineering, LLC. Material model calibration. Retrieved from <https://bit.ly/33iQ1uc> ; 20 August, 2019.
- [21] Sagar DS, Jeevan JJ, Ashish AS, et al. Shock absorber test set-up. *International Journal of Advance Engineering and Research Development*, 2017; 4(03): 690-698.
- [22] ASTM International. ASTM D575-91: Standard test methods for rubber properties in compression. Retrieved from <https://bit.ly/2OigmVh> ; 25 November, 2019.
- [23] Majid S, Ali K, Muhammad ZS, Muhammad F. Mechanical characterization and FE modelling of a hyperelastic material. *Journal of Material Research*, 2015; 18(5): 918-924.
- [24] 7075-T6 Aluminium. Retrieved from <https://www.makeitfrom.com/material-properties/7075-T6-Aluminium>; 25 November, 2019.
- [25] Robert HS. Analysing friction in the design of rubber products and their paired surfaces. 1st ed. Florida: CRC Press; 2008.
- [26] Bergström JS. Advanced user material subroutines for polymers. Retrieved from <https://bit.ly/2XFtC4y>; 25 November 2019.